

# Transparent boundary conditions for the elastic waves in anisotropic media

**Ivan L. Sofronov, Nickolai A. Zaitsev**

Keldysh Institute of Applied Mathematics RAS, Moscow

## Outline

- Problem formulation
- Generation of LRBC operator, main steps
- Numerical tests
- Conclusions

# Motivation

Generation of low-reflecting boundary conditions on open boundaries for anisotropic elastodynamics is a challenging problem. The PML method is not stable in this case, see

- *Beaches E., Fauqueux S., Joly P., Stability of perfectly matched layers group velocities and anisotropic waves, JCP, 188, 2003, 399 – 433;*
- *D. Appelö and G. Kreiss, A New Absorbing Layer for Elastic Waves, JCP, 215, 2006, 642 – 660.*

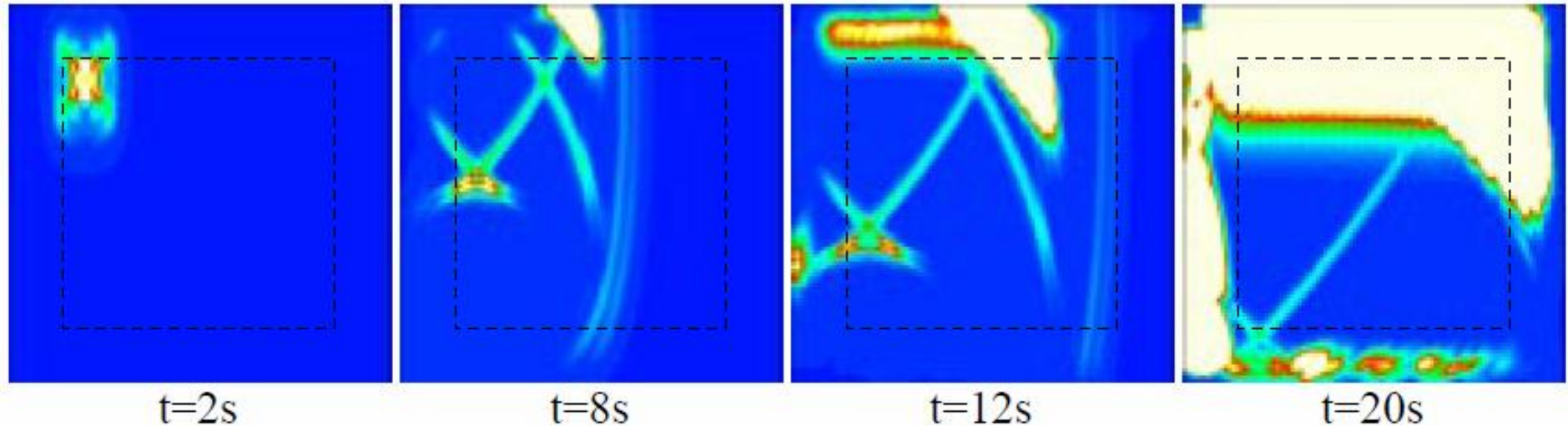
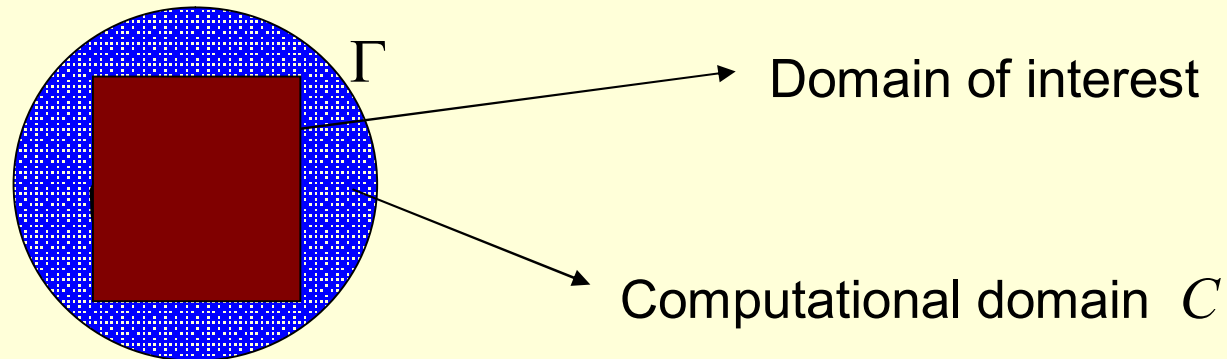


Figure 13: Some snapshots at different times for the orthotropic media (IV).

# Low-reflecting boundary conditions (LRBC)

LRBC on “open boundaries” are needed for modeling of wave propagation using a bounded computational domain.

Typical setup:



Generation of LRBC on  $\Gamma$  is an additional problem which is set up by considering auxiliary external Initial Boundary Value Problems (IBVPs) outside  $C$ .

*Remark:* In the domain of interest the governing equations and geometry can be much more complex than outside  $C$ .

# Anisotropic elasticity, 2D orthotropic media

We consider 2D elastodynamic equations:

$$\rho \frac{\partial^2 v_1}{\partial t^2} = c^{11} \frac{\partial^2 v_1}{\partial x_1^2} + c^{33} \frac{\partial^2 v_1}{\partial x_2^2} + (c^{33} + c^{12}) \frac{\partial^2 v_2}{\partial x_1 \partial x_2},$$
$$\rho \frac{\partial^2 v_2}{\partial t^2} = c^{33} \frac{\partial^2 v_2}{\partial x_1^2} + c^{22} \frac{\partial^2 v_2}{\partial x_2^2} + (c^{33} + c^{12}) \frac{\partial^2 v_1}{\partial x_1 \partial x_2}.$$

Here  $\rho$  is density;  $(v_1, v_2)$  is the Cartesian velocities;  $\{c^{nm}\}$  are (constant) elastic coefficients of the Hook's law written in the matrix form,  $\sigma^n = c^{nm} \varepsilon_m$ .

In polar coordinates for the velocity vector  $f = (v_r, v_\theta)$  the system reads:

$$\frac{\partial^2 f}{\partial t^2} = A^{11} \frac{\partial^2 f}{\partial r^2} + A^{22} \frac{\partial^2 f}{\partial \theta^2} + A^{12} \frac{\partial^2 f}{\partial r \partial \theta} + A^1 \frac{\partial f}{\partial r} + A^2 \frac{\partial f}{\partial \theta} + A^0 f$$

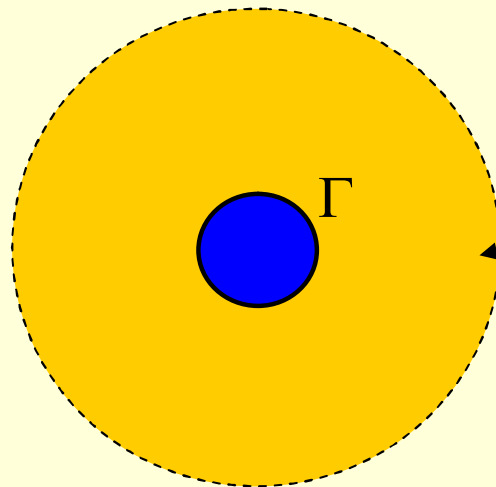
where  $A^{ij}(r, \theta)$ ,  $A^i(r, \theta)$  are 2x2 matrices

# Generation of LRBC operator, main steps

Governing equation in 2D space:  $f_{tt} - Lf = 0$

*Main steps:*

*Stage 1:* consider a set of auxiliary external IBVPs outside  $C$  (set wrt “ $m$ ”):



$$\begin{cases} \mathcal{E}^m_{tt} - L\mathcal{E}^m = 0 & \text{in } R^2 / C \\ \mathcal{E}^m|_{t=0} = 0 \\ \mathcal{E}^m|_{\Gamma} = \delta(t)\varphi^m(\theta) \end{cases} \quad (1)$$

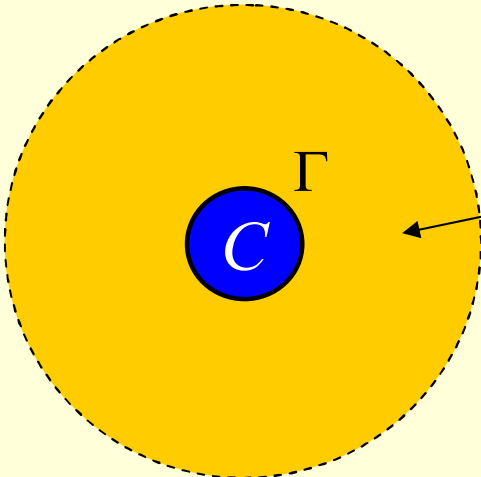
where  $\delta(t)$  is Dirac's delta function;

$\{\varphi^m(\theta)\}_{m=0}^{\infty}$  is a basis on  $\Gamma$ , i.e.  $f(t, \theta) = \sum_m c^m(t)\varphi^m(\theta)$

(in 2D it is constructed, e.g., by using  $\{\sin k\theta, \cos k\theta\}$  )

## Generation of LRBC operator (cont.)

Stage 2: make Laplace transform and pass to elliptic BVPs (parameterized by  $s$ ):



The diagram shows a large yellow circle representing the domain  $R^2 / C$ . Inside it is a smaller blue circle labeled  $C$ . The boundary of the yellow circle is marked with  $\Gamma$ . An arrow points from the boundary  $\Gamma$  to the boundary conditions in the equation below.

$$\begin{cases} s^2 \hat{\mathcal{E}}^m - L \hat{\mathcal{E}}^m = 0 & \text{in } R^2 / C \\ \hat{\mathcal{E}}^m |_{\Gamma} = \varphi^m(\theta) \\ \hat{\mathcal{E}}^m |_{r \rightarrow \infty} = 0 \end{cases} \quad (2)$$

Stage 3: solve (numerically) the problems and evaluate  $\frac{\partial}{\partial n} \hat{\mathcal{E}}^m(r, \theta)$  on  $\Gamma$

Thus we obtain the Dirichlet-to-Neumann maps

$$\varphi^m(\theta) \mapsto \psi^m(\theta)[s] \quad \left( \equiv \frac{\partial}{\partial n} \hat{\mathcal{E}}^m(\theta, r), r = R_{\Gamma} \right)$$

# Generation of LRBC operator (cont.)

Stage 4: form matrix of the Poincare-Steklov operator:

we take arbitrary data on  $\Gamma$

$$\hat{f}(s, \theta) = \sum_m \hat{c}^m(s) \varphi^m(\theta)$$

and write the representation of its normal derivative on  $\Gamma$

$$\frac{\partial}{\partial n} \hat{f}(s, \theta) = \sum_m \hat{c}^m(s) \psi^m(\theta)[s] = \sum_m \hat{c}^m(s) \sum_n P_n^m(s) \varphi^n(\theta)$$

Thus we obtain the Poincare-Steklov operator in space of Fourier coefficients:

$$\hat{d}^n(s) = \sum_m \hat{P}_n^m(s) \hat{c}^m(s) \quad \left( \frac{\partial}{\partial n} \hat{f}(s, \theta) = \sum_n \hat{d}^n(s) \varphi^n(\theta) \right)$$

or, in matrix form:

$$\hat{\mathbf{d}}(s) = \hat{\mathbf{P}}(s) \hat{\mathbf{c}}(s), \quad \hat{\mathbf{c}} = \left\{ \hat{c}^0, \hat{c}^1, \dots \right\}^T$$

# Generation of LRBC operator (cont.)

*Stage 5:* make inverse Laplace transform for the P-S operator.

**First** we represent matrix  $\hat{\mathbf{P}}(s)$  by sum of three matrices to take into account asymptotic at  $s \rightarrow \infty$ :

$$\hat{\mathbf{P}}(s) = \mathbf{P}_1 s + \mathbf{P}_0 + \hat{\mathbf{K}}(s); \quad \mathbf{P}_1, \mathbf{P}_0 \text{ are } \textit{consts}, \quad \hat{\mathbf{K}}(s) = o(1)$$

**Then** we calculate rational approximations to each entry in  $\hat{\mathbf{K}}(s)$  such that all poles have negative real parts, i.e.

$$\hat{K}_n^m(s) \approx \tilde{K}_n^m(s) \equiv \sum_{l=1}^{L_n^m} \frac{\alpha_{n l}^m}{s - \beta_{n l}^m}, \quad \text{Re}(\beta_{n l}^m) \leq \delta < 0$$

**Finally** the inverse Laplace transform of  $\hat{\mathbf{d}}(s) = \hat{\mathbf{P}}(s)\hat{\mathbf{c}}(s)$  gives:

$$\mathbf{d}(t) = \mathbf{P}_1 \frac{\partial \mathbf{c}(t)}{\partial t} + \mathbf{P}_0 \mathbf{c}(t) + \tilde{\mathbf{K}}(t) * \mathbf{c}(t)$$



## Generation of LRBC operator (cont.)

*Remark:* the explicit form of kernels  $\tilde{K}_n^m(t)$  is

$$\tilde{K}_n^m(t) = \sum_{l=1}^{L_n^m} \alpha_{n,l}^m \exp(\beta_{n,l}^m t), \quad \text{Re}(\beta_{n,l}^m) \leq \delta < 0$$

that permits to treat convolutions by stable recurrent formulas.

*Stage 6:* compose azimuth modes:

Denote by  $\mathbf{Q}$  the operator of Fourier decomposition for  $f(t, \theta) = \sum_m c^m(t) \varphi^m(\theta)$

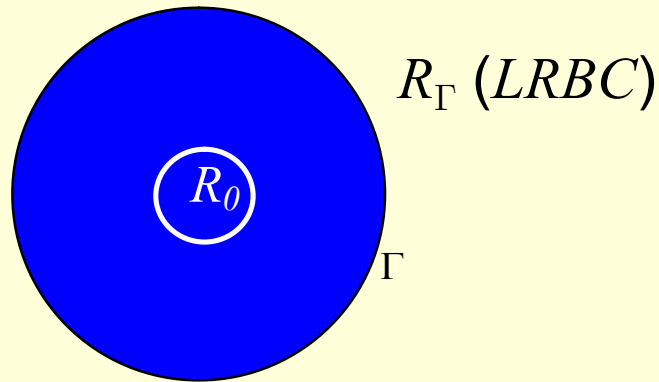
i.e.  $\mathbf{Q}: f(t, \theta) \rightarrow \{c^m(t)\}$ . Consequently,  $\mathbf{Q}^{-1}: \{c^m(t)\}, \{d^m(t)\} \rightarrow f, \frac{\partial f}{\partial n}$

The LRBC in the physical space reads:

$$\mathbf{Q}^{-1} \mathbf{P}_1 \mathbf{Q} \frac{\partial f}{\partial t} - \frac{\partial f}{\partial n} + \mathbf{Q}^{-1} \mathbf{P}_0 \mathbf{Q} f + \mathbf{Q}^{-1} \{ \tilde{\mathbf{K}}(t) * \} \mathbf{Q} f = 0$$

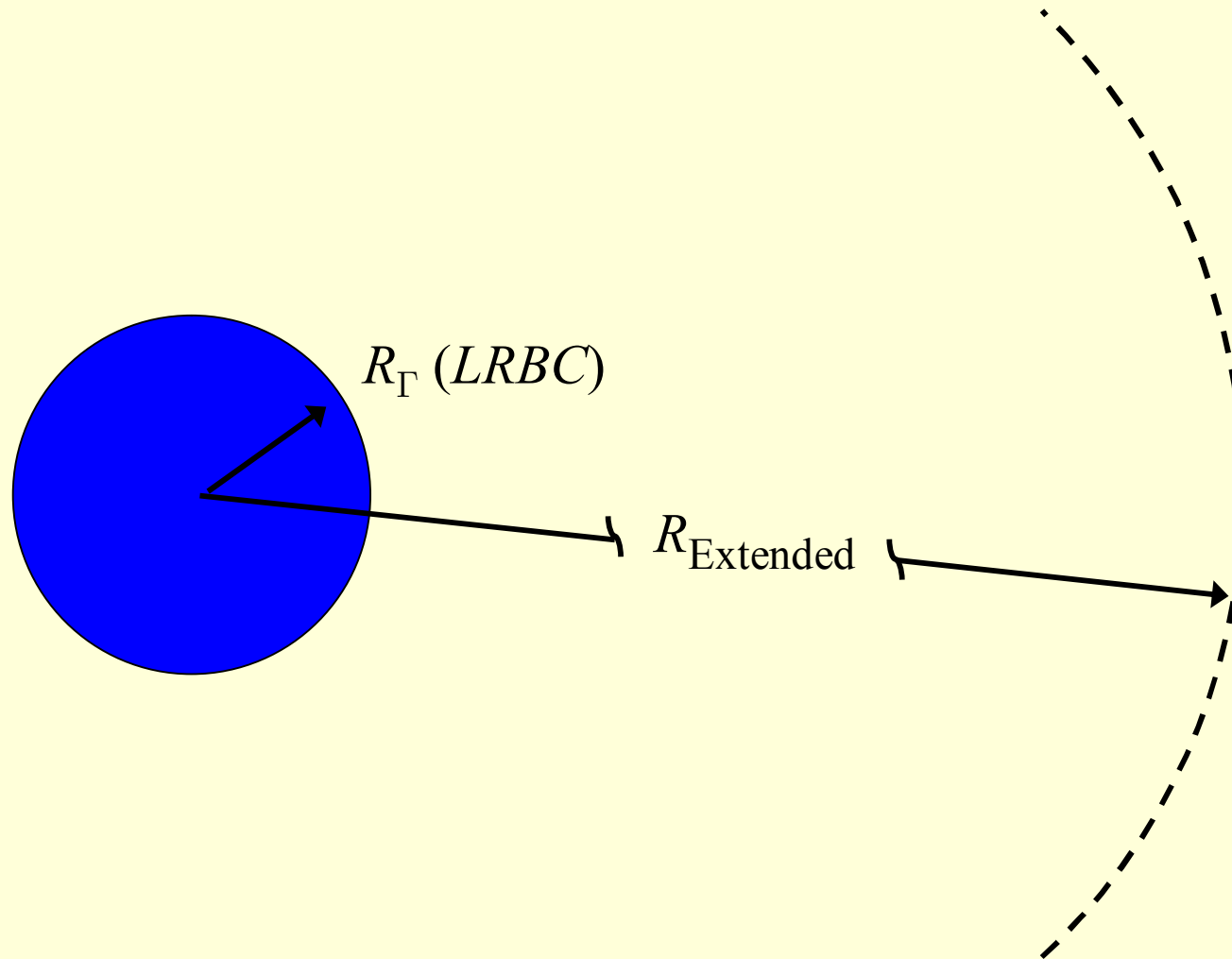
# Setup of the test problem

Governing equations are implemented in the polar system of coordinates. We consider the task in a circle:



- At  $R_0 = 2$  we prescribe Dirichlet data (pulse) to initiate elastic waves;
- $\Gamma$  with radius  $R_\Gamma = 10$  is the external boundary where we put LRBC (with 36 azimuth harmonics).

# Test problem: reference solution



The verification of LRBC is made by comparing with the *reference solution* of a second problem having  $\delta x$  bigger external radius (extended domain).

Comparison of two solutions in  $C$ -norm is made at  $r < R_\Gamma$ .

# Test calculations

Parameters of anisotropic media are taken from

*Beaches E., Fauqueux S., Joly P., Stability of perfectly matched layers group velocities and anisotropic waves, JCP, 188, 2003, 399 – 433:*

anisotropic medium, case IV:  $c_{11} = 4, \quad c_{22} = 20, \quad c_{33} = 2, \quad c_{12} = 7.5$

$$\rho \frac{\partial^2 v_1}{\partial t^2} = c^{11} \frac{\partial^2 v_1}{\partial x_1^2} + c^{33} \frac{\partial^2 v_1}{\partial x_2^2} + (c^{33} + c^{12}) \frac{\partial^2 v_2}{\partial x_1 \partial x_2},$$

$$\rho \frac{\partial^2 v_2}{\partial t^2} = c^{33} \frac{\partial^2 v_2}{\partial x_1^2} + c^{22} \frac{\partial^2 v_2}{\partial x_2^2} + (c^{33} + c^{12}) \frac{\partial^2 v_1}{\partial x_1 \partial x_2}.$$

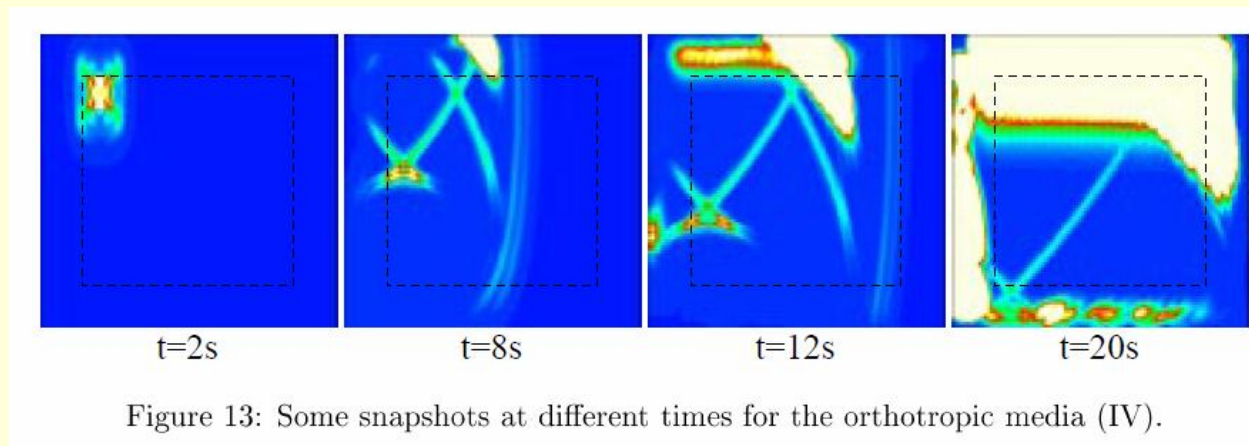
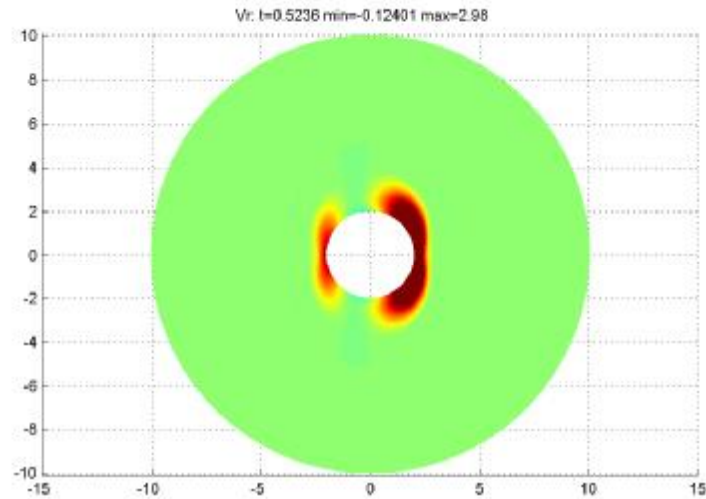


Figure 13: Some snapshots at different times for the orthotropic media (IV).

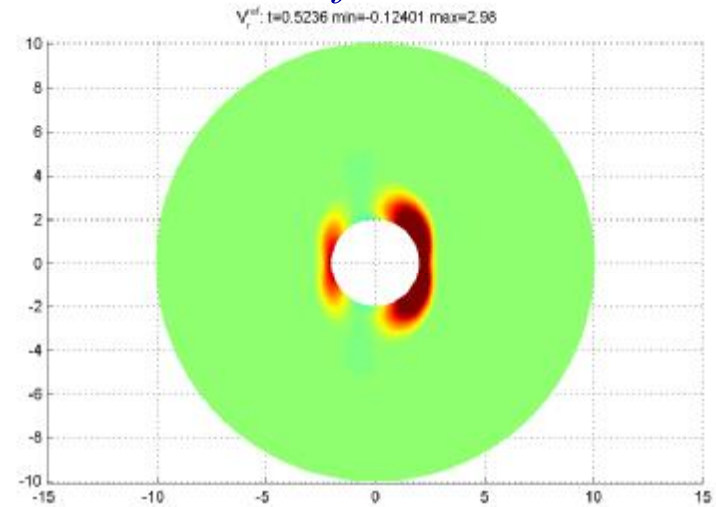
# Anisotropic case-IV, $t=0.52$

$U_r$

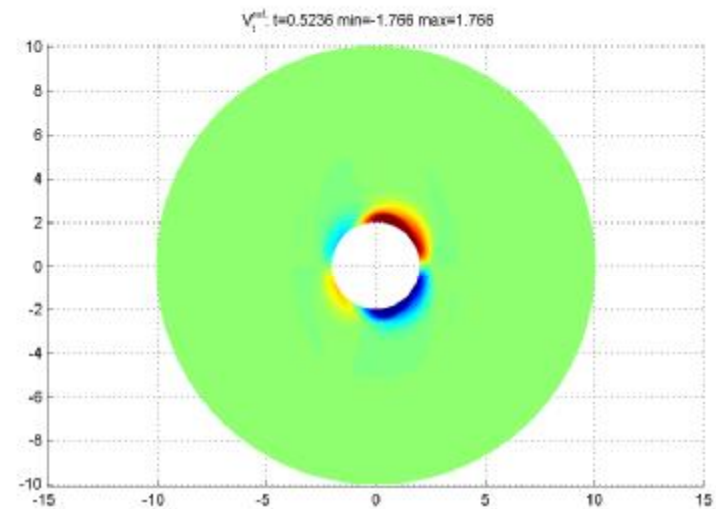
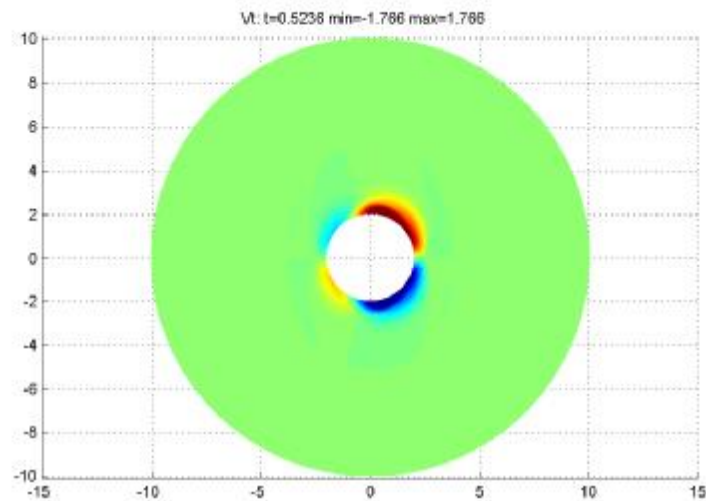
*LRBC*



*Reference*



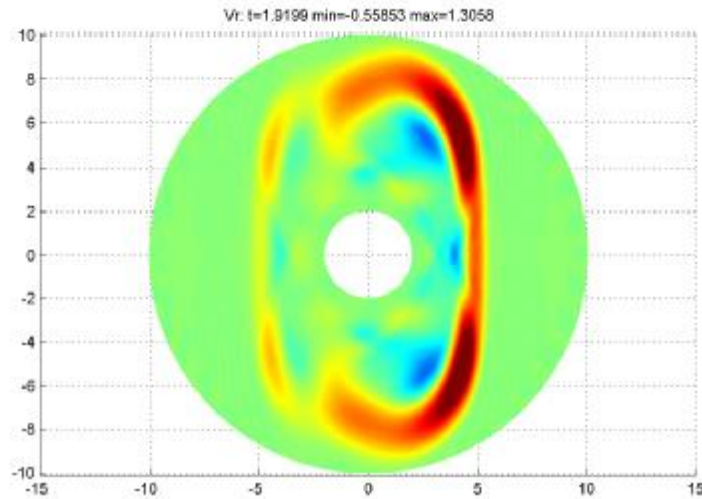
$U_{theta}$



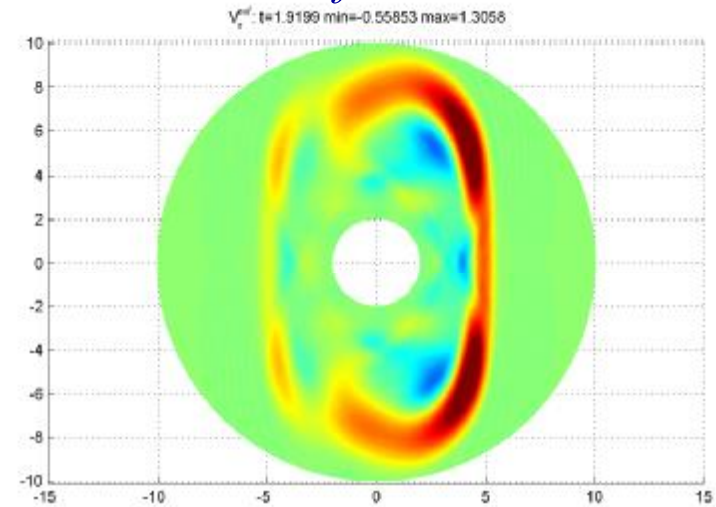
# Anisotropic case-IV, $t=1.92$

$U_r$

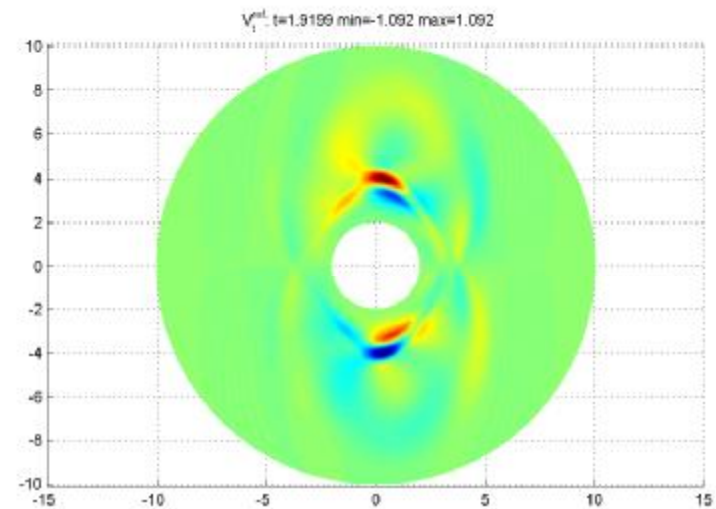
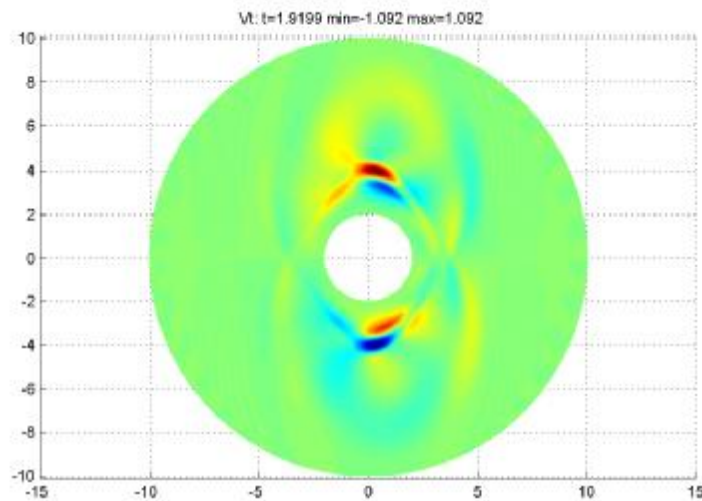
*LRBC*



*Reference*



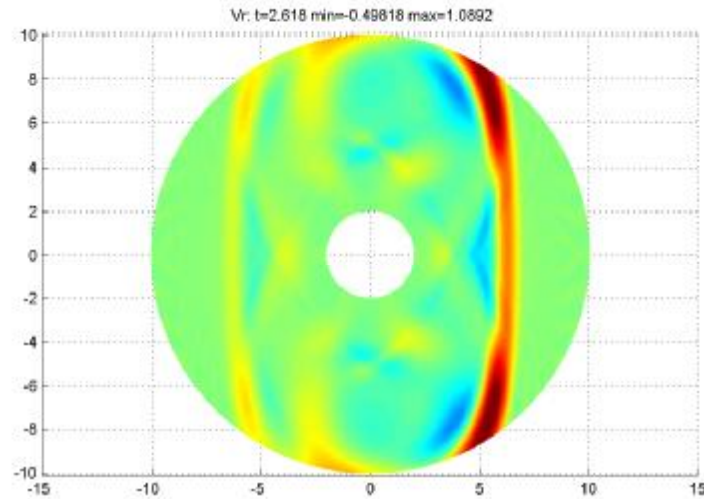
$U_{\theta}$



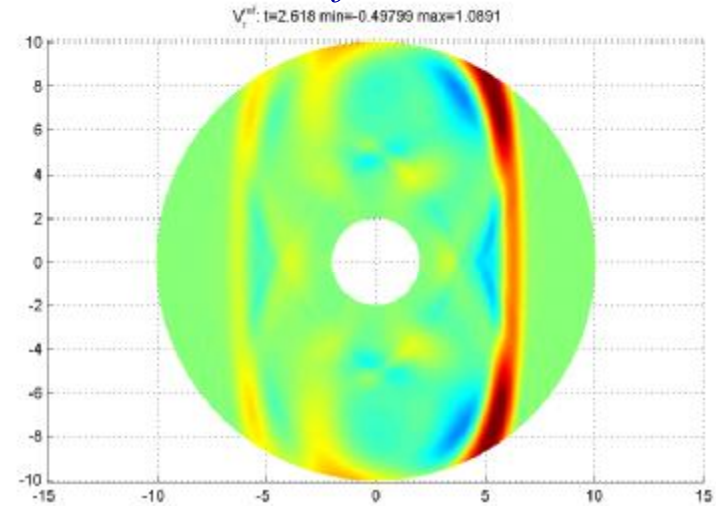
# Anisotropic case-IV, $t=2.62$

$U_r$

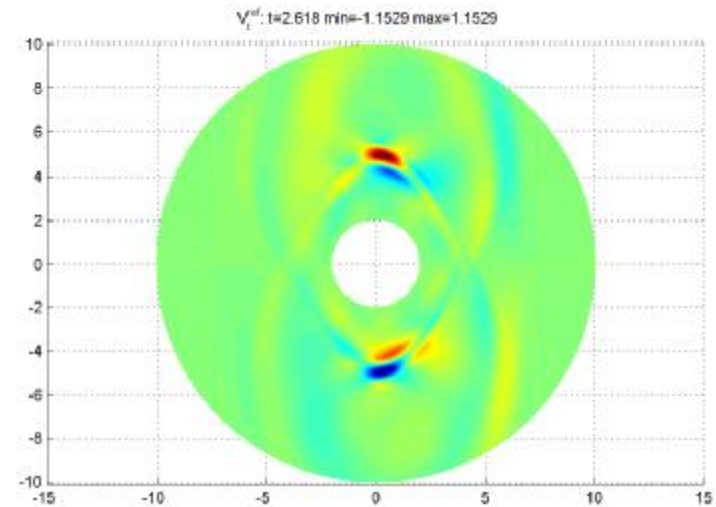
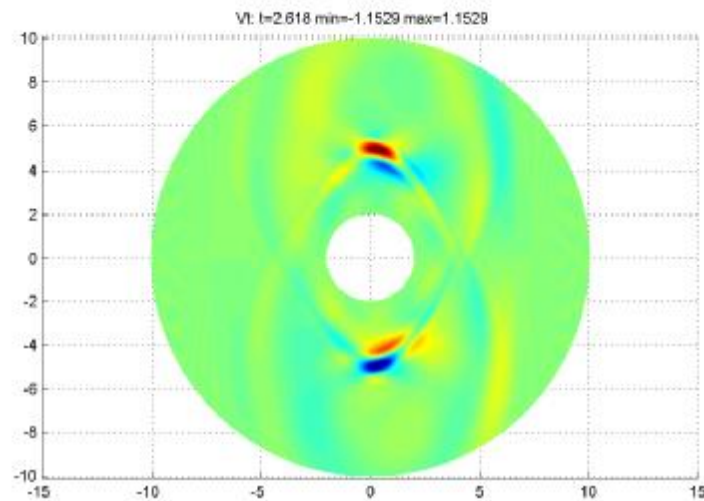
*LRBC*



*Reference*



$U_{theta}$

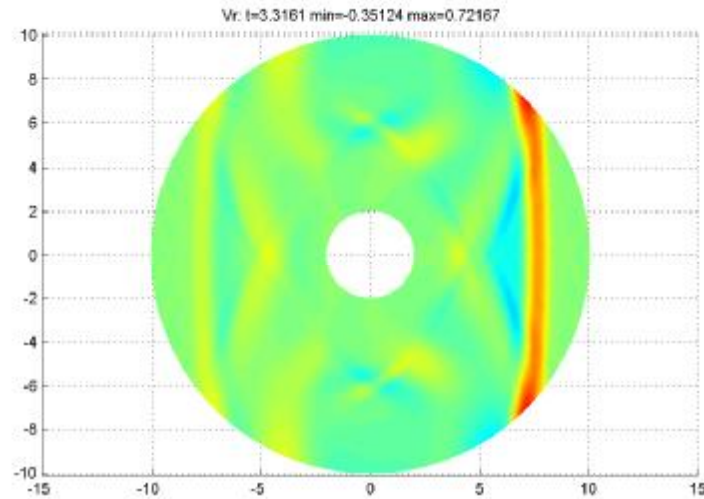




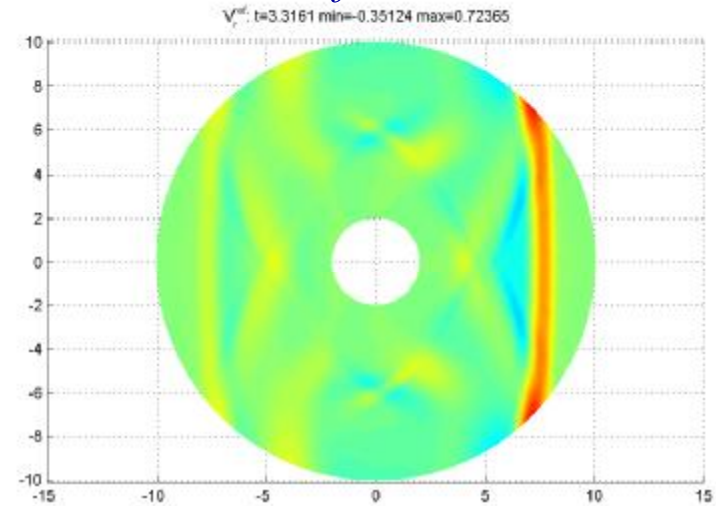
# Anisotropic case-IV, $t=3.32$

$U_r$

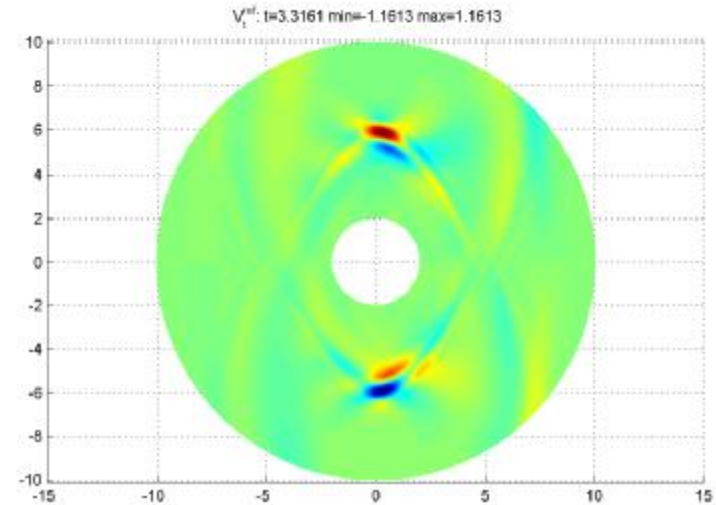
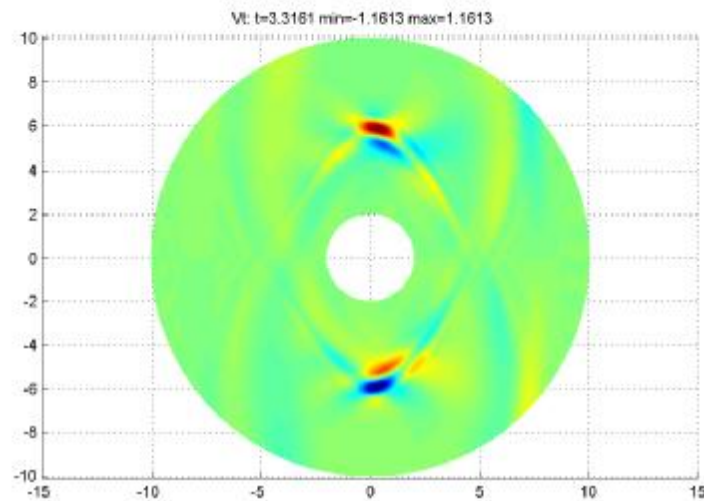
*LRBC*



*Reference*



$U_{theta}$

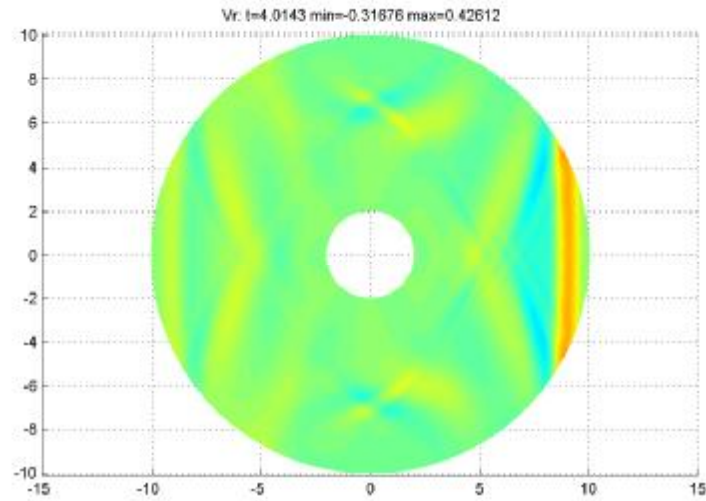




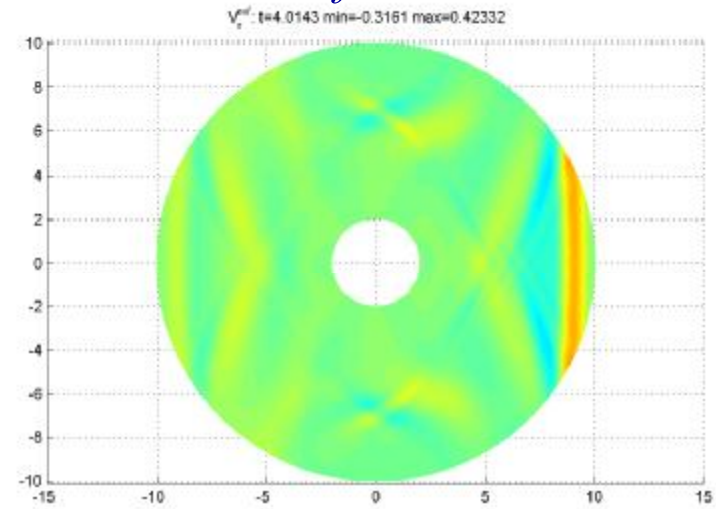
# Anisotropic case-IV, $t=4.01$

$U_r$

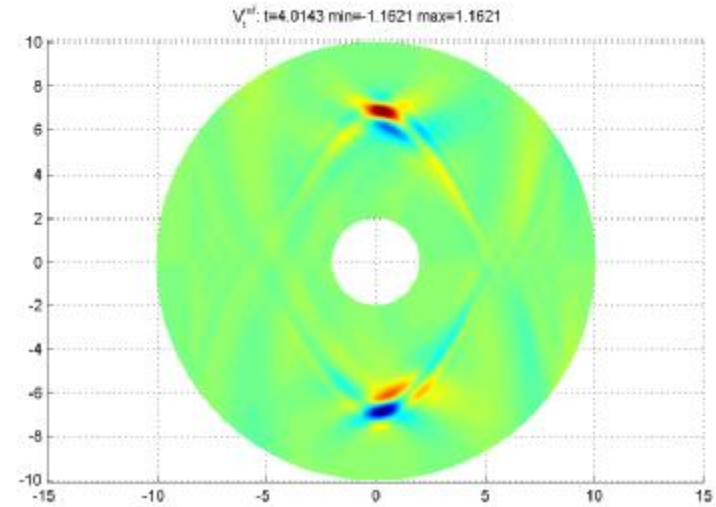
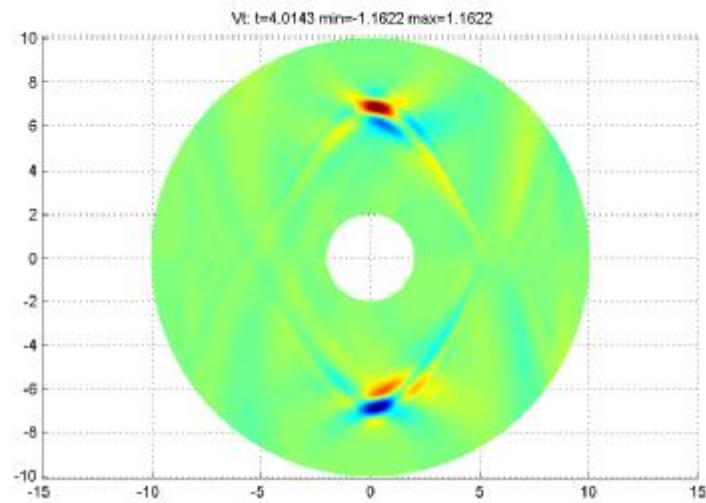
*LRBC*



*Reference*



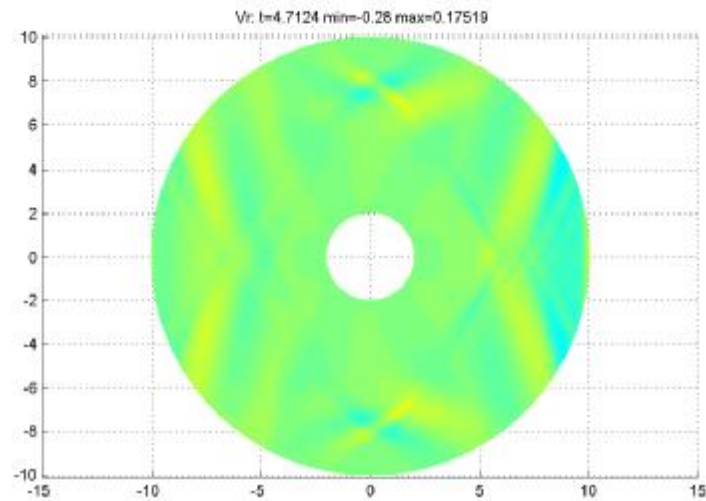
$U_{theta}$



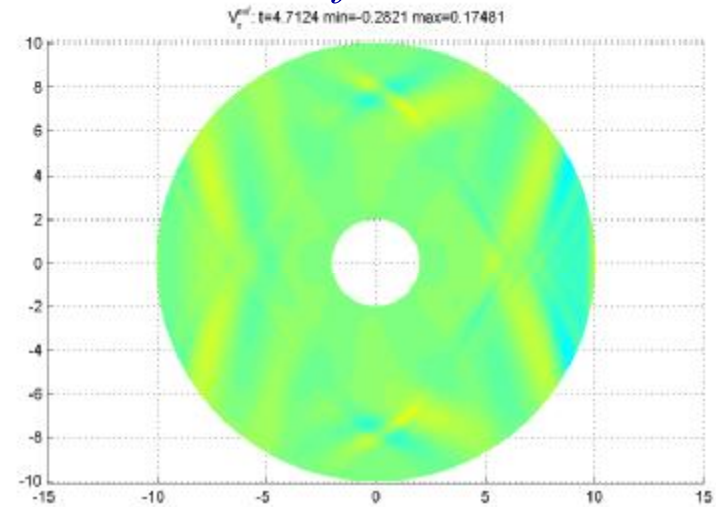
# Anisotropic case-IV, $t=4.71$

$U_r$

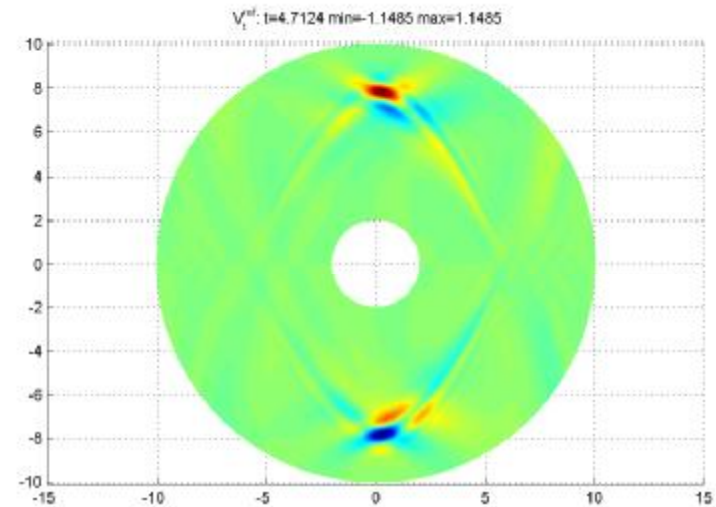
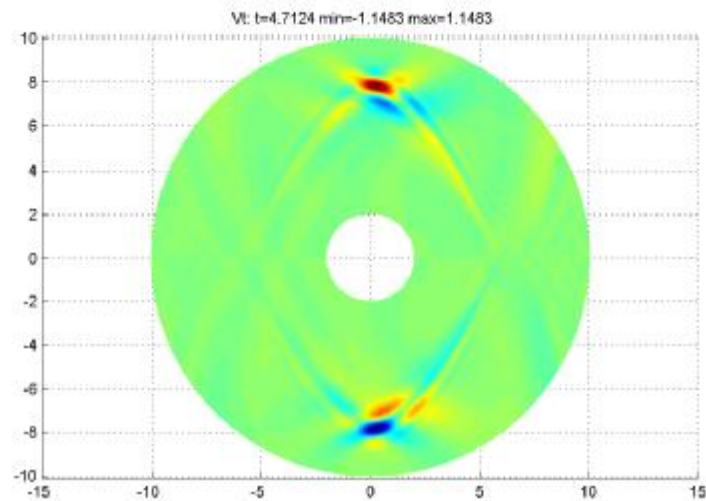
*LRBC*



*Reference*



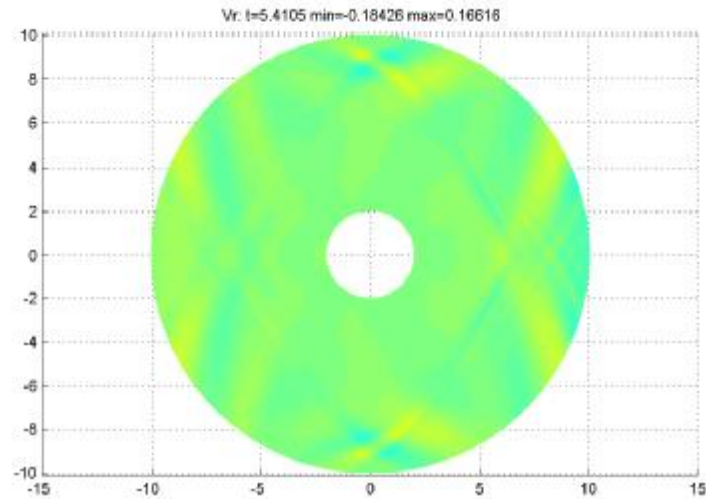
$U_{theta}$



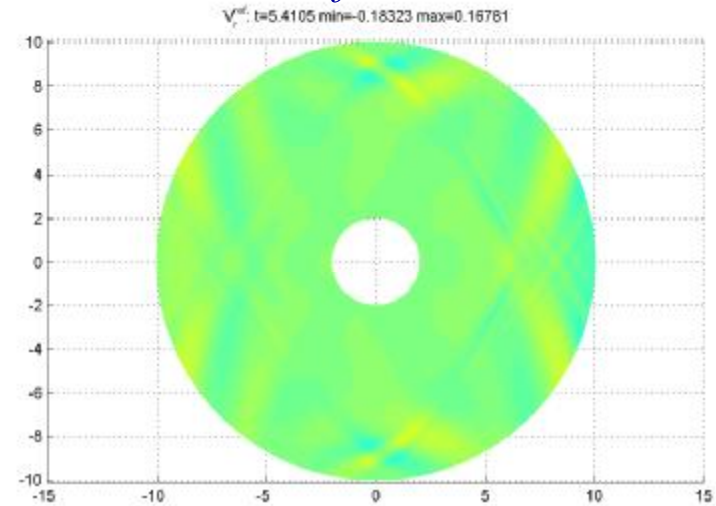
# Anisotropic case-IV, $t=5.41$

$U_r$

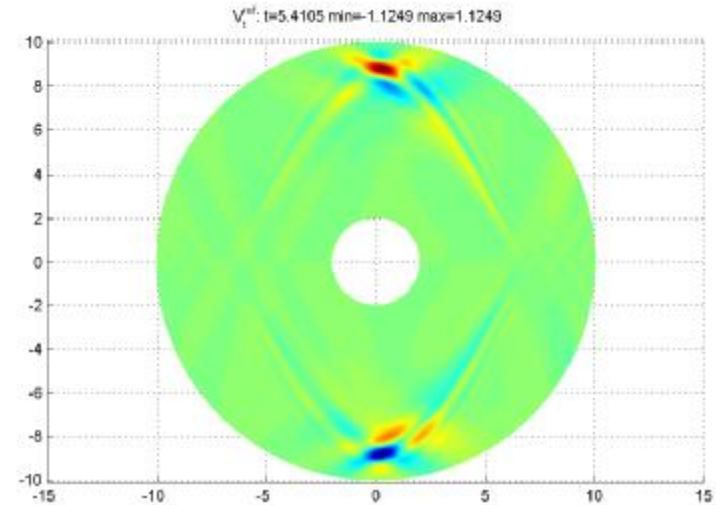
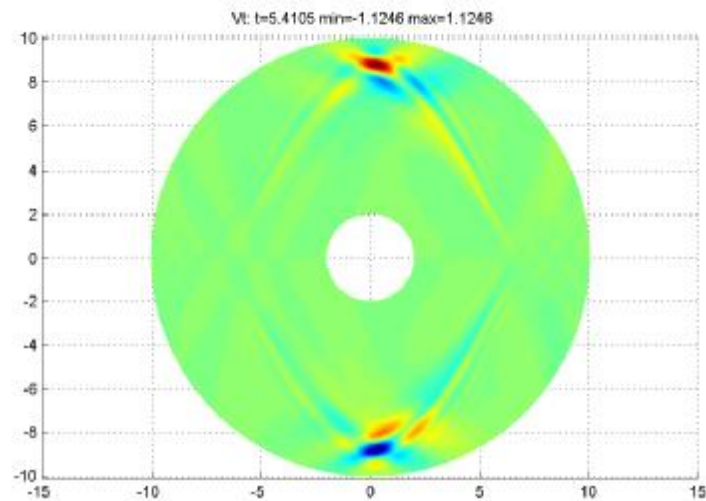
*LRBC*



*Reference*



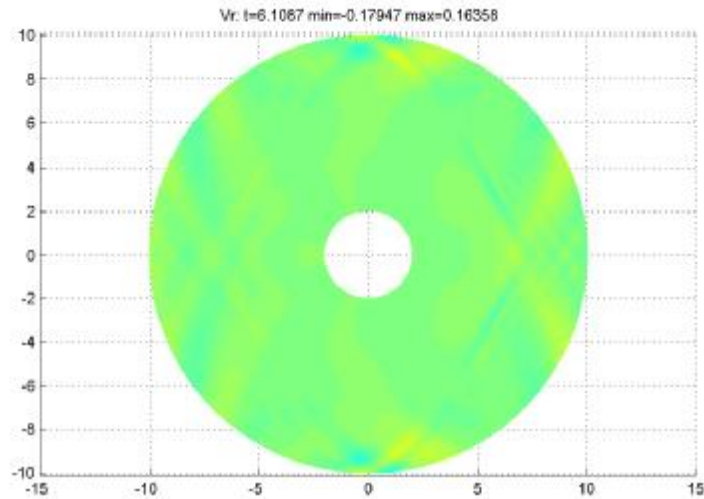
$U_{theta}$



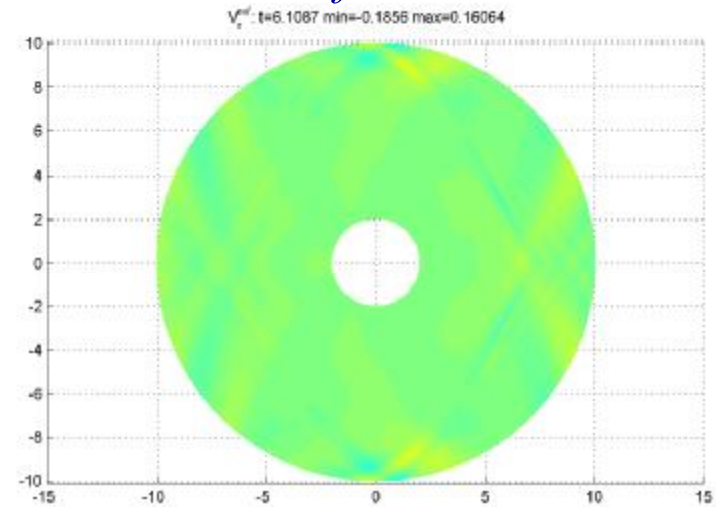
# Anisotropic case-IV, $t=6.11$

$U_r$

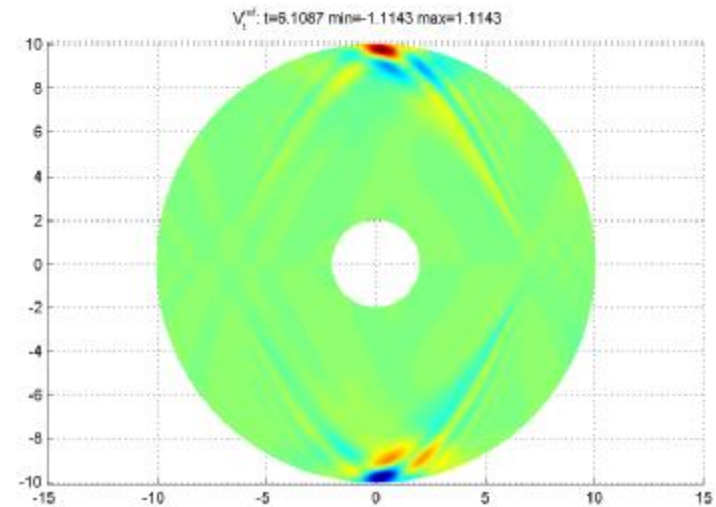
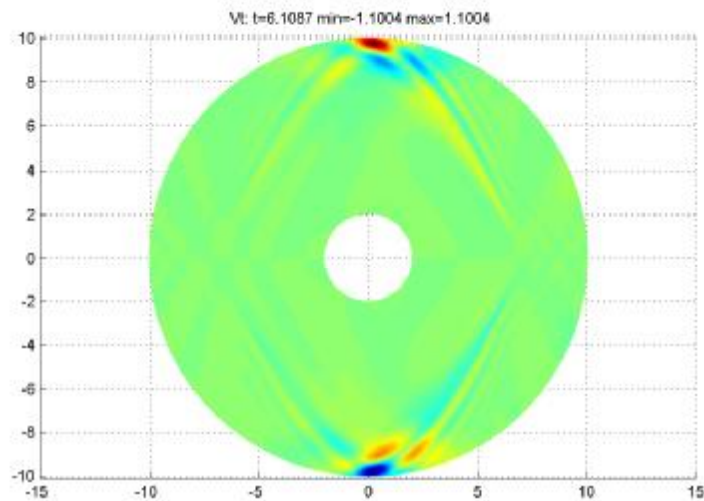
*LRBC*



*Reference*



$U_{theta}$

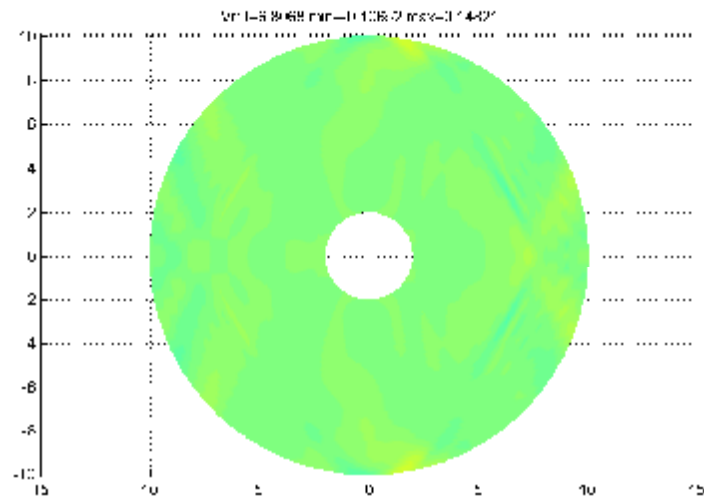




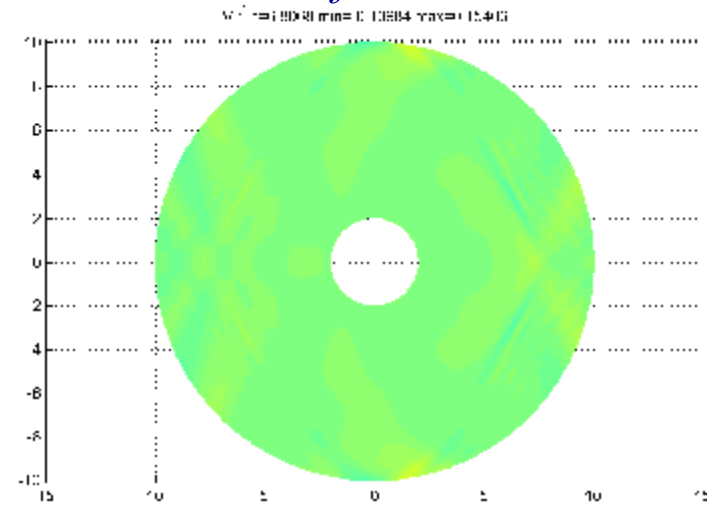
# Anisotropic case-IV, $t=6.81$

$U_r$

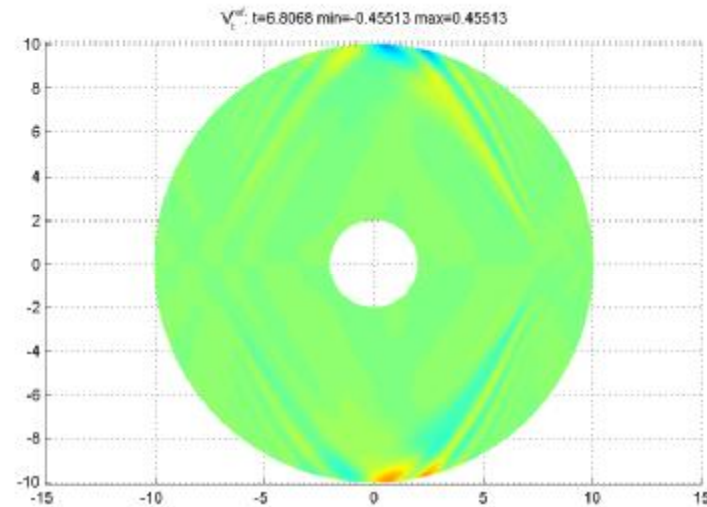
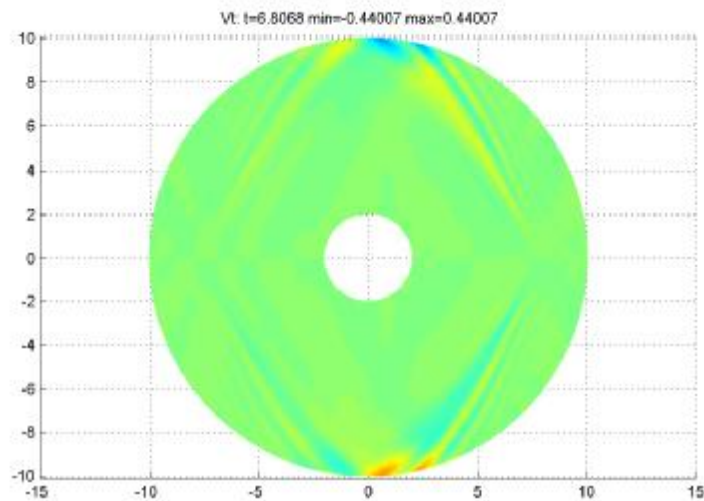
*LRBC*



*Reference*



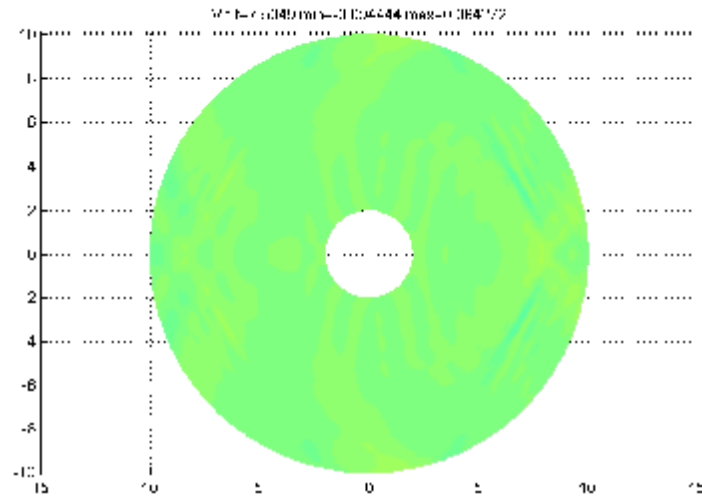
$U_{theta}$



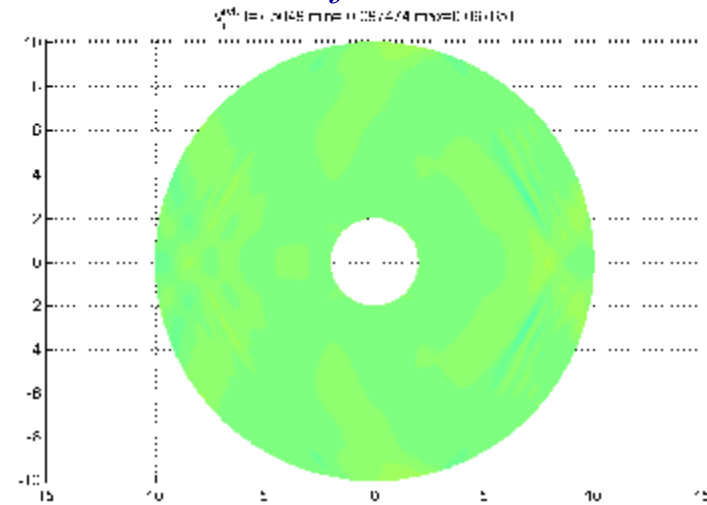
# Anisotropic case-IV, $t=7.50$

$U_r$

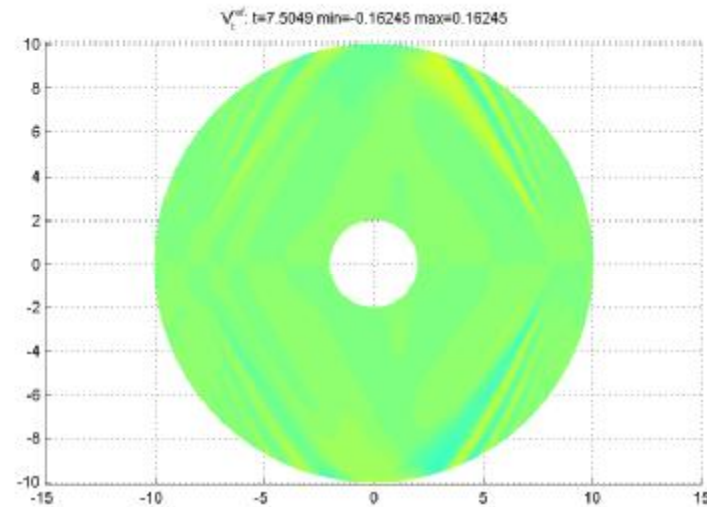
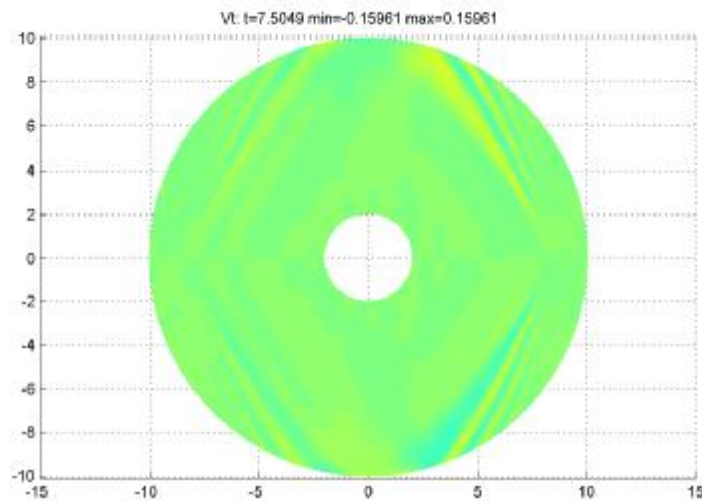
*LRBC*



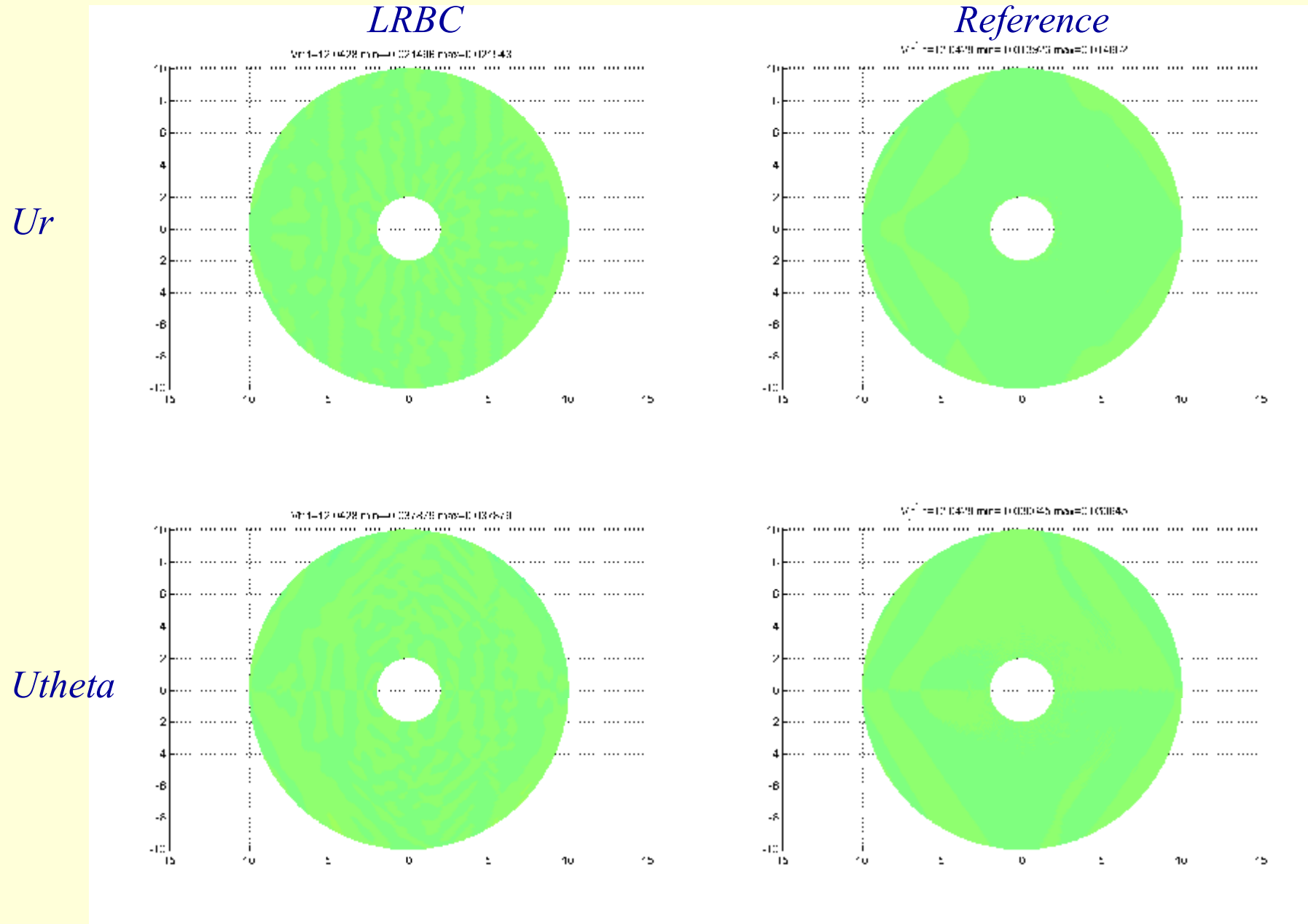
*Reference*



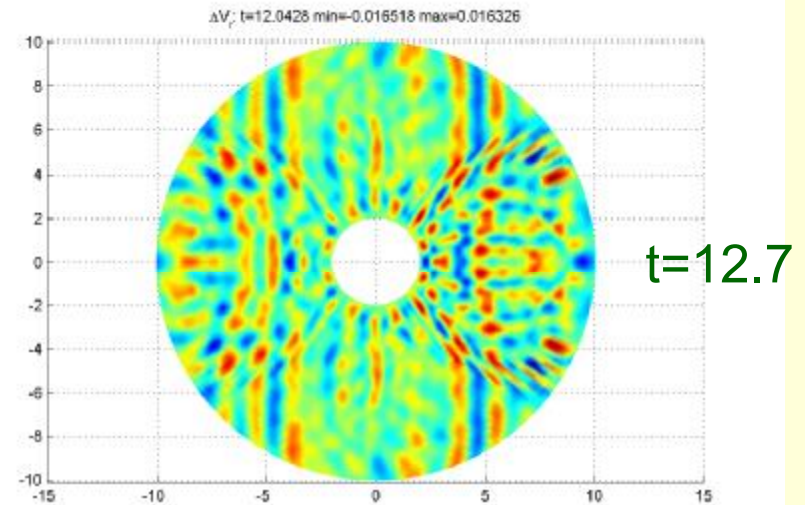
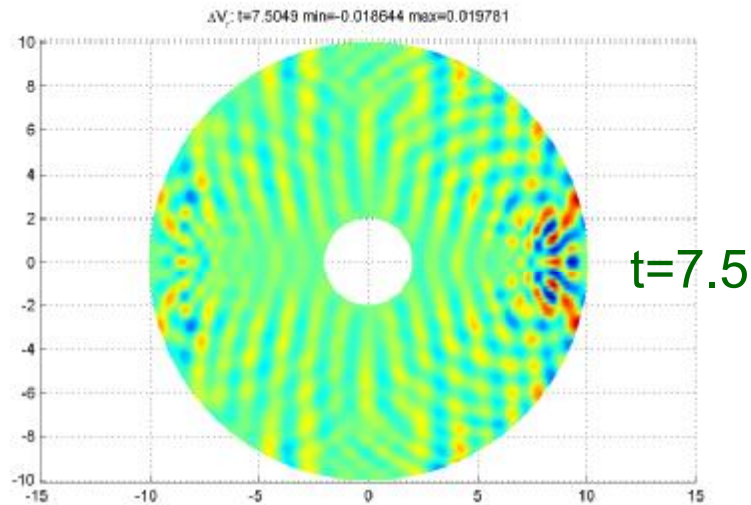
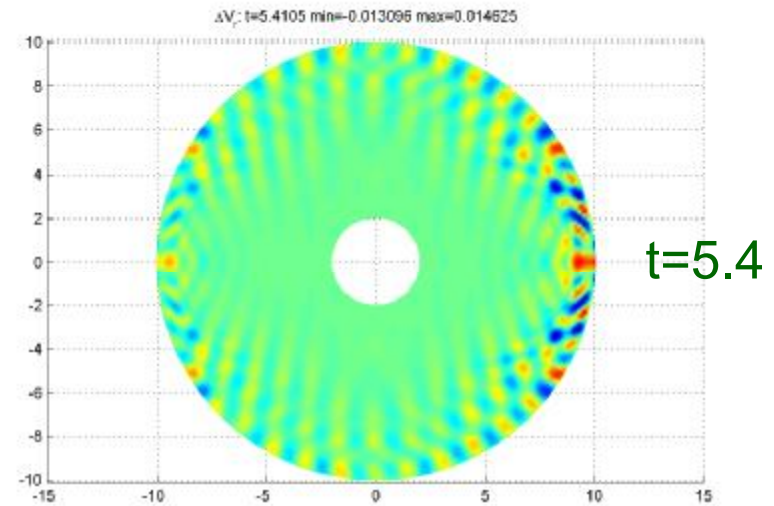
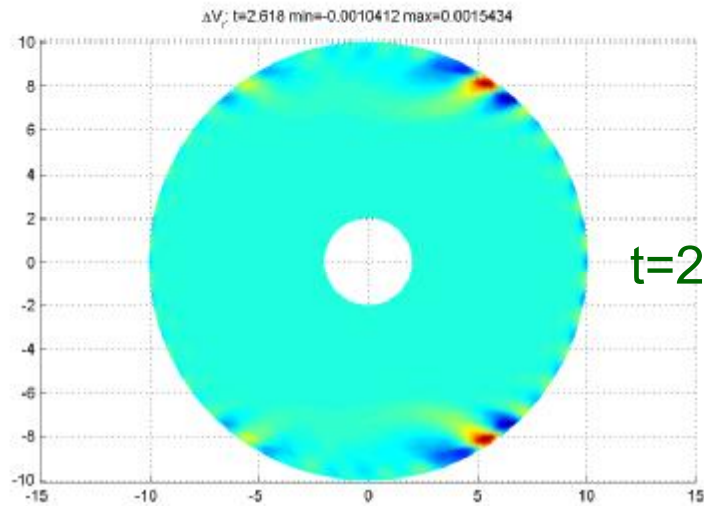
$U_{theta}$



# Anisotropic case-IV, $t=12.0$

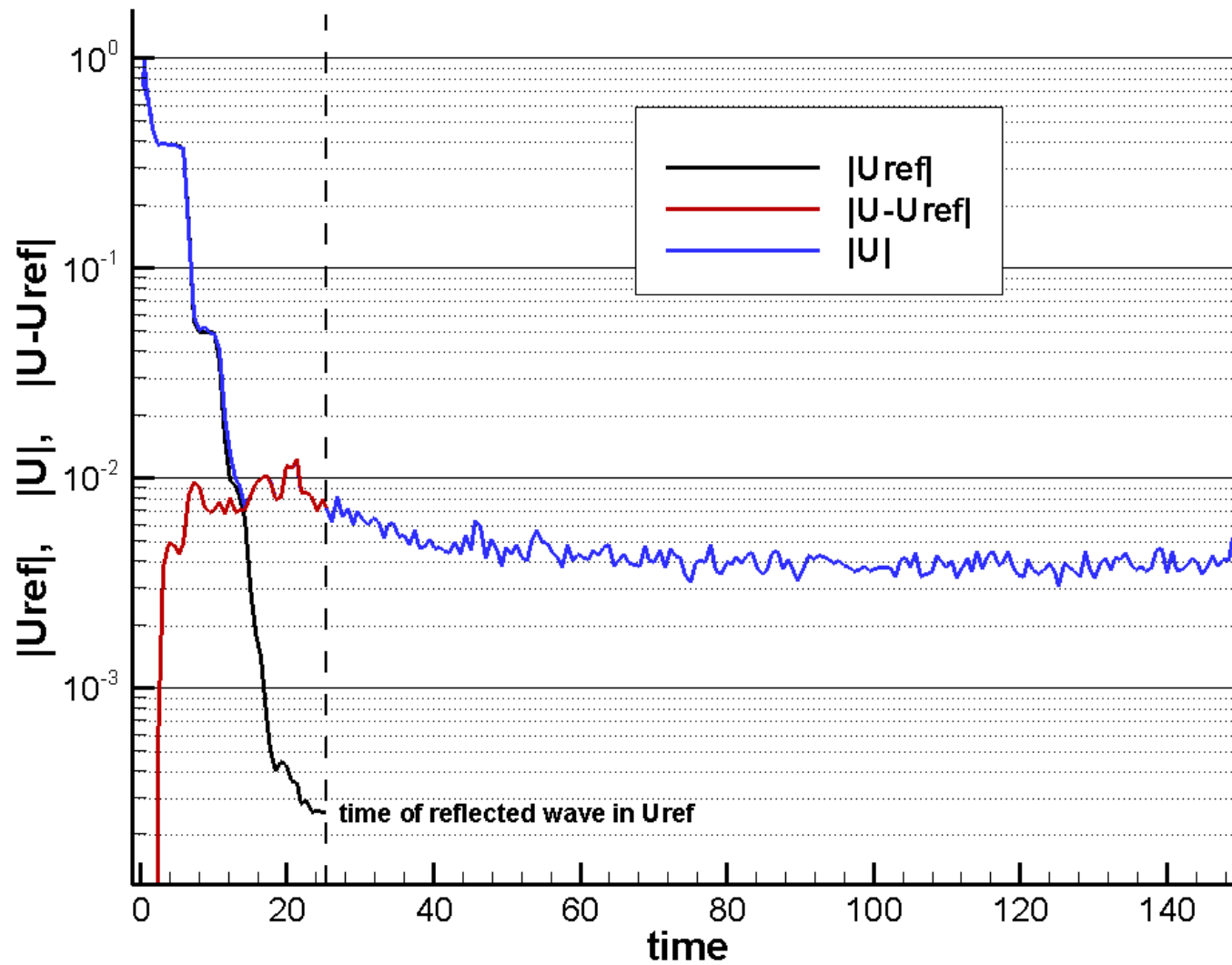


# Difference between LRBC and Reference solution





# LRBC stability at large times



# Conclusions

- A novel approach to generate numerical LRBCs for anisotropic time-domain wave propagation problems is proposed and implemented in 2D
- LRBCs are efficient in both isotropic and anisotropic media, including the case where PML approach fails (case IV)
- LRBC operator does not depend on the meshing inside the computational domain
- LRBC efficiency (amplitude of reflected waves) can be automatically controlled during generation of the operator
- It is possible to generate in advance a library of LRBC matrices for given media parameters and geometry of computational domain
- The algorithm is highly parallelized

# Further research

- The approach is still computationally expensive and must be revised and improved to enhance the performance
- Real\*16 accuracy
- 3D problems

# LRBC operator, numerical aspects

Main features of the algorithm for *discretized system*:

*Stages 1–6*: we take discrete azimuth basis  $\{\sin k\theta, \cos k\theta\}, k = 0, 1, \dots, M; (M = 20)$ ;

*Stage 2 [Laplace image]*: we take a finite interval

$[0, S_{\max}]$  and choose set of knots  $\{s_j\} \in [0, S_{\max}]$

which are representative enough to consider

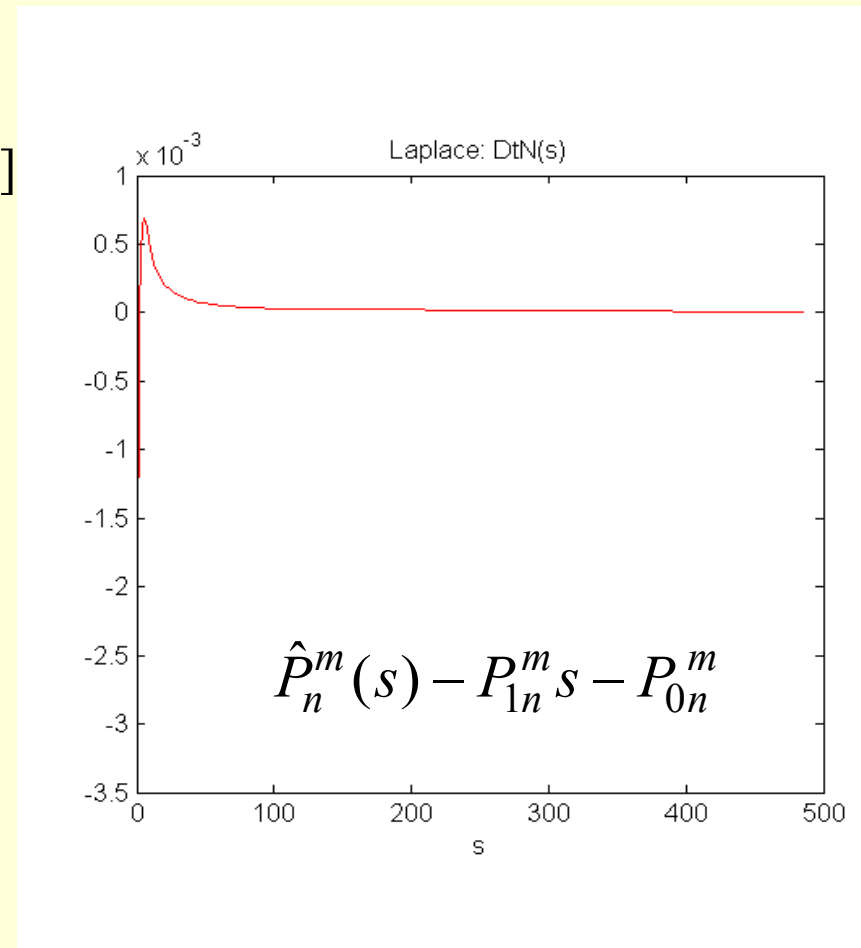
discrete counterparts of kernels  $\hat{P}_n^m(s_j)$

for rational approximation (Stage 5).

In particular, the Chebyshev's nodes are used:

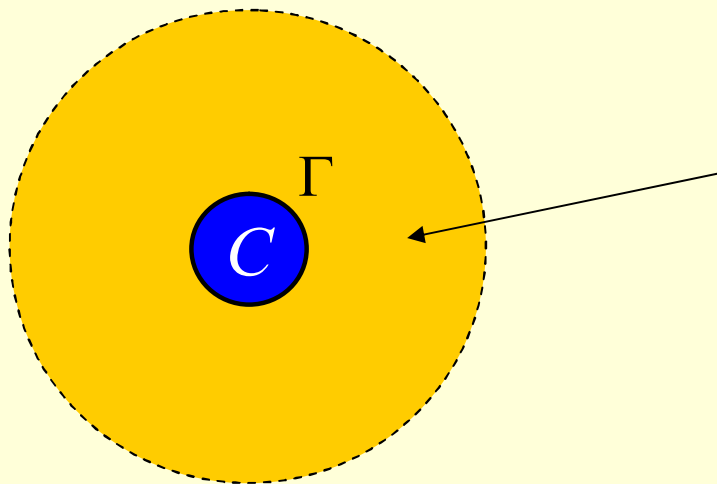
$$s_j = \frac{S_{\max}}{2} \left( 1 - \cos \left( \pi \frac{j - 0.5}{J} \right) \right), \quad j = 1, \dots, J$$

$J \sim 100$



# LRBC operator, numerical aspects (cont.)

Stages 3-4 [*P-S operator*]: we discretise governing equations by *pseudospectral* derivatives in azimuth direction (uniform grid) and *finite differences* in radial direction (exponential grid) and make massive calculations to evaluate each  $\hat{P}_n^m(s_j)$  with a guaranteed accuracy,  $\varepsilon_{PS} \sim 10^{-10}$  (controlled by mesh convergence). Number of separate tasks is  $4 * (M + 1) * J$ ;


$$\begin{cases} s^2 \hat{\mathcal{E}}^m - L \hat{\mathcal{E}}^m = 0 & \text{in } R^2 / C \\ \hat{\mathcal{E}}^m |_{\Gamma} = \varphi^m(\theta) \\ \hat{\mathcal{E}}^m |_{r \rightarrow \infty} = 0 \end{cases}$$

Thus we form the matrix  $\hat{\mathbf{P}}(s_j)$ .

# LRBC operator, numerical aspects (cont.)

Stage 5 [inverse Laplace transform]:

Constant matrices  $\mathbf{P}_1, \mathbf{P}_0$  are estimated from the rational approximations

$$R_n^m(s_j) \approx \hat{P}_n^m(s_j)$$

on the interval  $[0, S_{\max}]$  ( $R_n^m(s)$  is calculated by Chebyshev-Pade algorithm), and the reminder matrix is formed:

$$\hat{\mathbf{K}}(s_j) := \hat{\mathbf{P}}(s_j) - \mathbf{P}_1 s_j - \mathbf{P}_0$$

Rational approximations are calculated for each  $\hat{K}_n^m(s_j)$  :

$$\left\| \sum_{l=1}^L \frac{\alpha_l}{s_j - \beta_l} - \hat{K}(s_j) \right\|_{\{s_j\}}^2 \rightarrow \min_{\alpha_l, \beta_l}, \quad \text{Re}(\beta_l) \leq \delta < 0$$

(indices  $\begin{smallmatrix} m \\ n \end{smallmatrix}$  at  $\hat{K}, L, \alpha, \beta$  are omitted);  $L=8$ .

The minimization is made by an optimization algorithm.

## LRBC operator, numerical aspects (cont.)

As a result we obtain the rational functions  $\hat{K}_n^m(s)$  satisfying

$$|\hat{K}_n^m(s_j) - \tilde{K}_n^m(s_j)| < \varepsilon_R \quad (\varepsilon_R \sim 10^{-8})$$

They are explicitly inverted from the Laplace space:

$$\hat{K}_n^m(s) \mapsto \tilde{K}_n^m(t) \equiv \sum_{l=1}^{L_n^m} \alpha_{n,l}^m \exp(\beta_{n,l}^m t), \quad \text{Re}(\beta_{n,l}^m) \leq \delta < 0$$

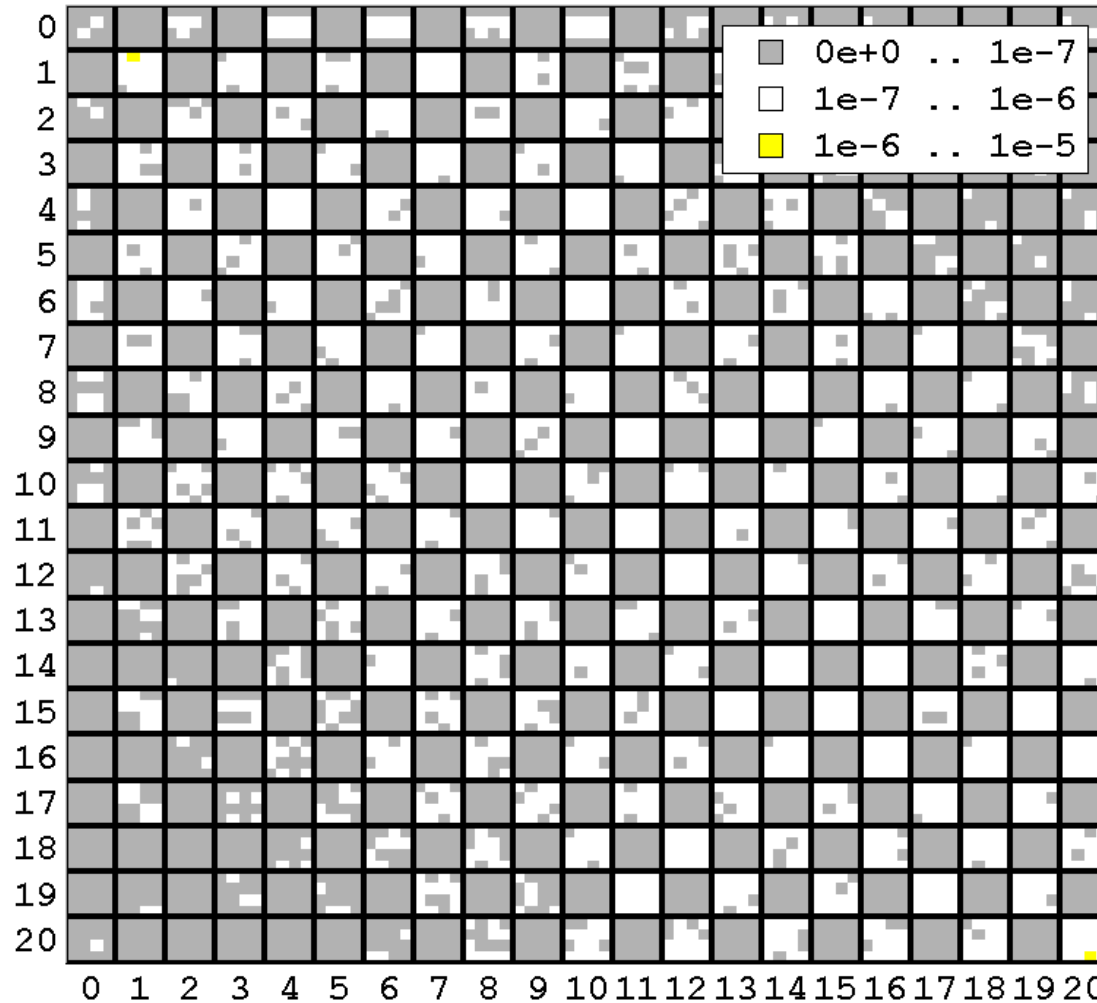
*Stage 6 [discrete NRBC]:* introducing matrices  $\mathbf{Q}_M^{-1}, \mathbf{Q}_M$  of the discrete Fourier transform for vector-functions  $f = (v_r, v_\theta)$  in *sin-cos* basis, we write out our discrete BC:

$$\mathbf{Q}_M^{-1} \mathbf{P}_1 \mathbf{Q}_M \frac{\partial f}{\partial t} - \frac{\partial f}{\partial n} + \mathbf{Q}_M^{-1} \mathbf{P}_0 \mathbf{Q}_M f + \mathbf{Q}_M^{-1} \{ \tilde{\mathbf{K}}(t) * \} \mathbf{Q}_M f = 0$$

*Remark:* in isotropic case  $\mathbf{P}_1 = p_1 \mathbf{I}$ ,  $\mathbf{P}_0 = p_0 \mathbf{I}$ ,  $\tilde{\mathbf{K}}(t)$  is diagonal

# LRBC matrix, residual $\max_{s_j} | \hat{K}_n^m(s_j) - \tilde{K}_n^m(s_j) |$

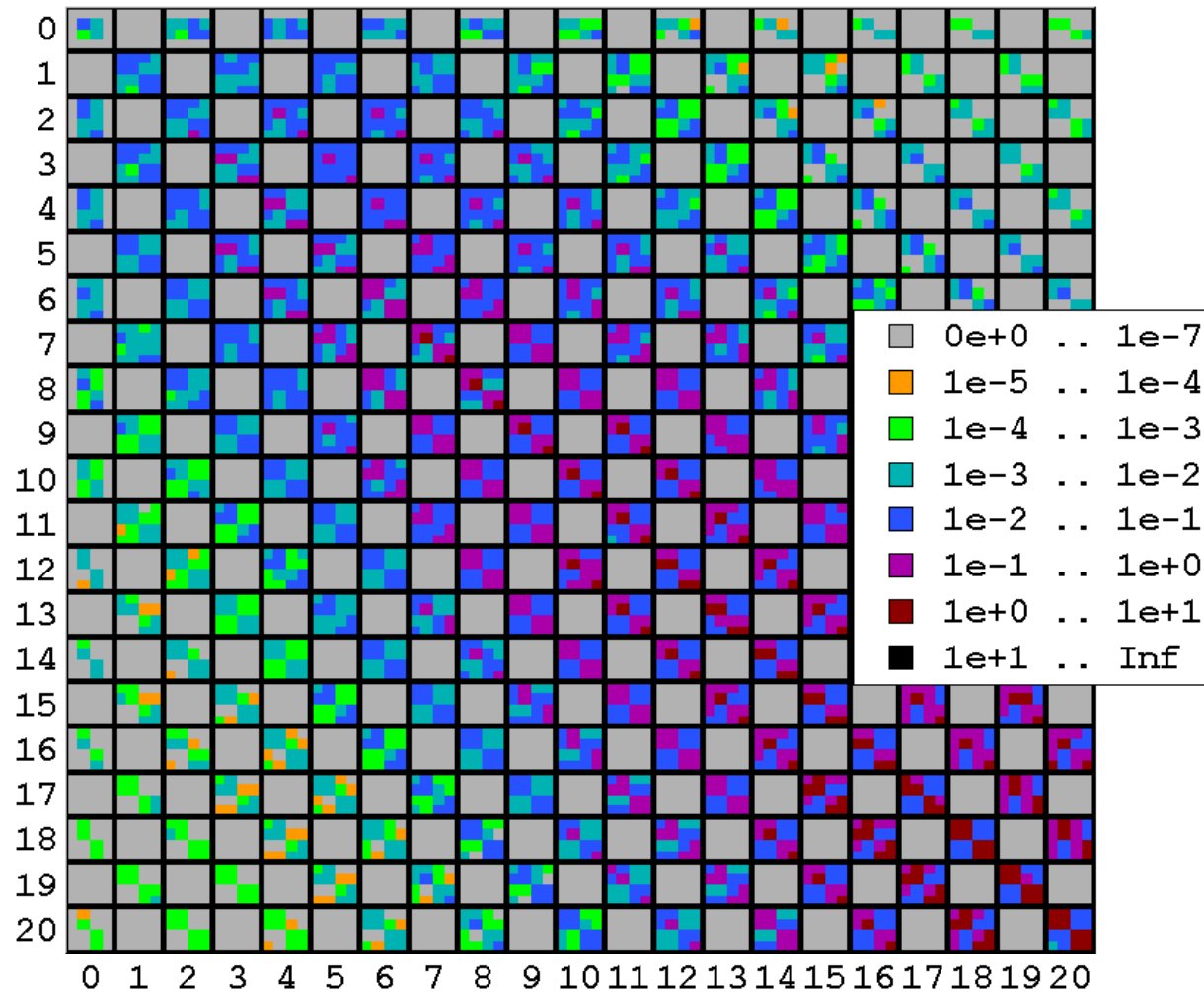
$$\mathbf{Q}_M^{-1} \mathbf{P}_1 \mathbf{Q}_M \frac{\partial f}{\partial t} - \frac{\partial f}{\partial n} + \mathbf{Q}_M^{-1} \mathbf{P}_0 \mathbf{Q}_M f + \mathbf{Q}_M^{-1} \{ \tilde{\mathbf{K}}(t) * \} \mathbf{Q}_M f = 0$$





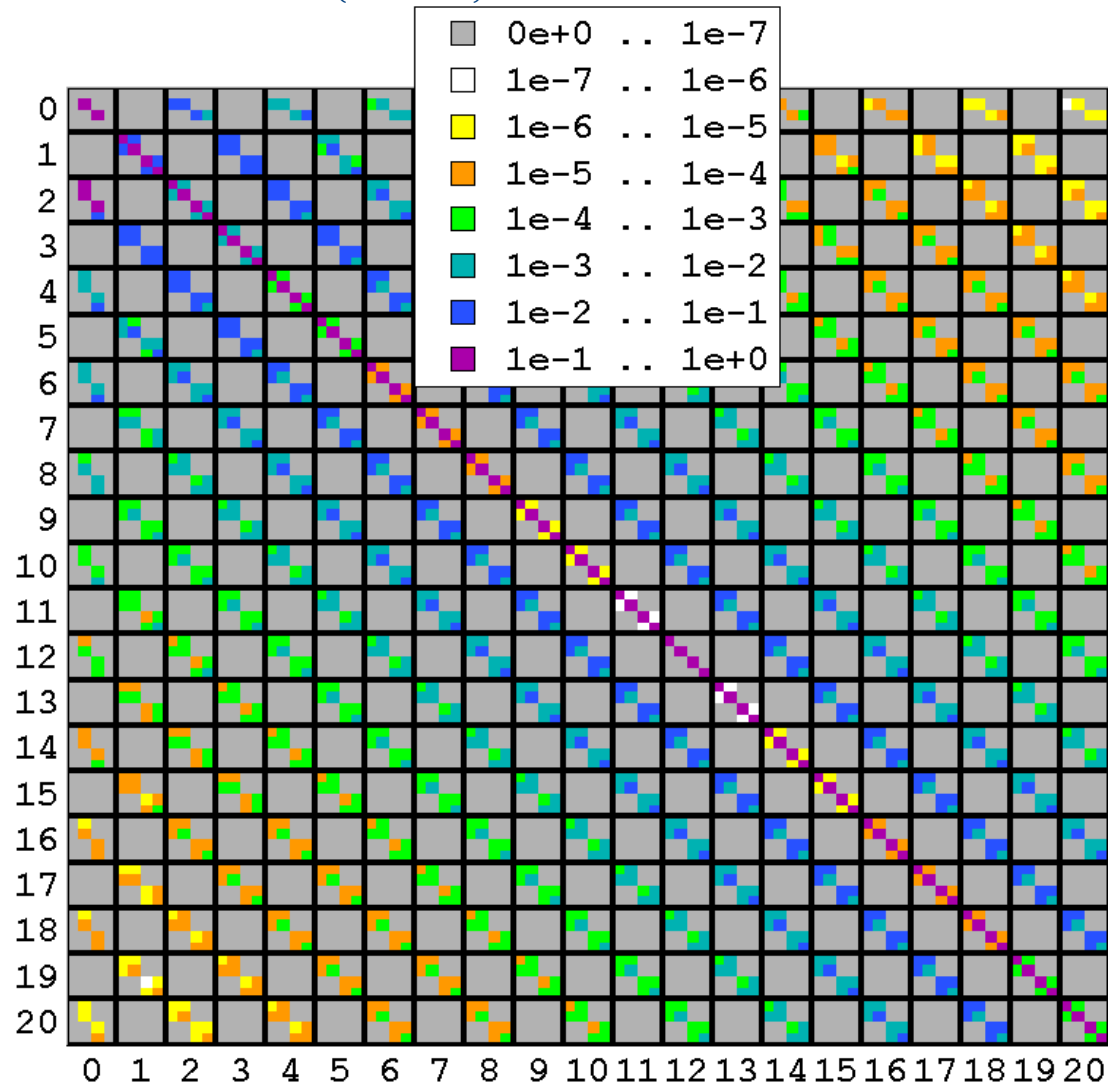
# LRBC matrix, amplitude $\max_t |\tilde{K}_n^m(t)|$

$$\mathbf{Q}_M^{-1} \mathbf{P}_1 \mathbf{Q}_M \frac{\partial f}{\partial t} - \frac{\partial f}{\partial n} + \mathbf{Q}_M^{-1} \mathbf{P}_0 \mathbf{Q}_M f + \mathbf{Q}_M^{-1} \{ \tilde{\mathbf{K}}(t) * \} \mathbf{Q}_M f = 0$$



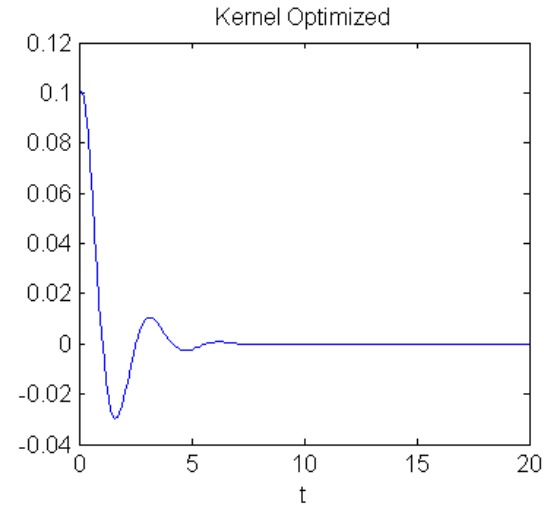
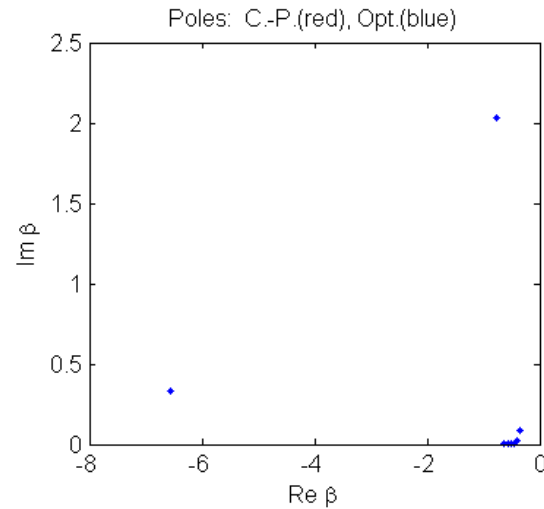
# LRBC matrix, amplitude $|P_{1n}^m|$

$$\mathbf{Q}_M^{-1} \mathbf{P}_1 \mathbf{Q}_M \frac{\partial f}{\partial t} - \frac{\partial f}{\partial n} + \mathbf{Q}_M^{-1} \mathbf{P}_0 \mathbf{Q}_M f + \mathbf{Q}_M^{-1} \{ \tilde{\mathbf{K}}(t) * \} \mathbf{Q}_M f = 0$$



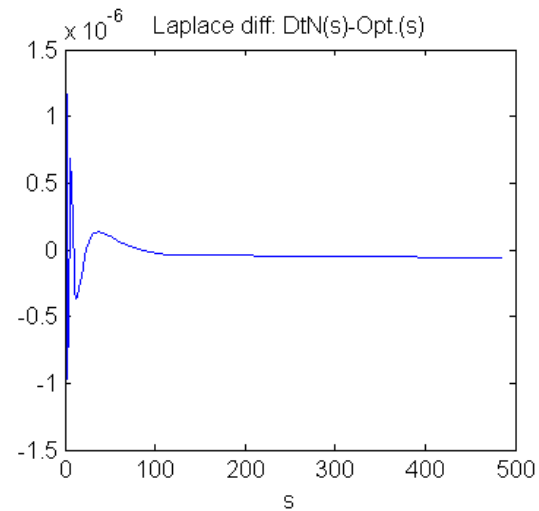
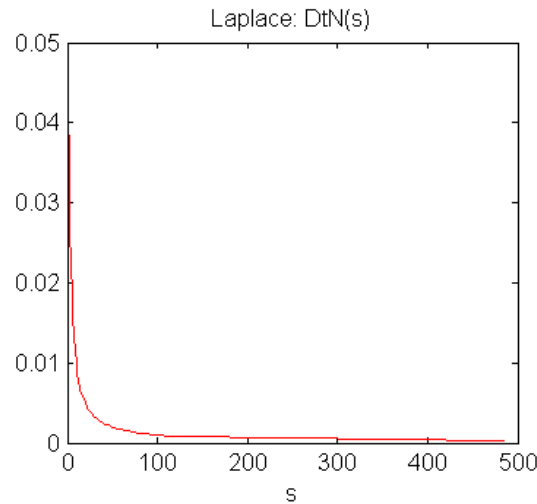
# LRBC matrix, entry $n = (14,1) \rightarrow m = (18,3)$

poles of  $\hat{K}_n^m(s)$



$\tilde{K}_n^m(t)$

$\hat{K}_n^m(s)$



$\hat{K}_n^m(s) - \tilde{K}_n^m(s)$